Common methods of making giant vesicles (except emulsion techniques) capture intended lipid ratios

Heidi M.J. Weakly[1†], Kent J. Wilson[1†], Gunnar J. Goetz[1], Emily L. Pruitt[1], Amy Li[2], Libin Xu[2] and Sarah L. Keller[1*]

[1] Department of Chemistry, University of Washington, Seattle, WA, 98195
[2] Department of Medicinal Chemistry, University of Washington, Seattle, WA, 98195

Keywords: lipid, vesicle, liposome, mass spectrometry
Running title: Most vesicle lipid ratios are correct

† These two authors contributed equally
* Corresponding author: slkeller@uw.edu

ORCID:

H.M.J. Weakly	0000-0001-8594-6337
K.J. Wilson	0009-0000-6206-9300
G.J. Goetz	0000-0002-5316-7950
E.L. Pruitt	0000-0001-9522-4311
A. Li	0000-0002-7732-3540
L. Xu	0000-0003-1021-5200
S.L. Keller	0000-0001-5919-0185

ABSTRACT:

Researchers choose different methods of making giant unilamellar vesicles in order to satisfy different constraints of their experimental designs. A challenge of using a variety of methods is that each may produce vesicles of different lipid compositions, even if all vesicles are made from a common stock mixture. Here, we use mass spectrometry to investigate ratios of lipids in giant vesicles made by four common methods: electroformation on indium tin oxide slides, electroformation on platinum wires, gentle hydration, and emulsion transfer. The vesicles are made from a mixture of common lipid types: di(18:1)PC, di(16:0)PC, di(18:1)PG, di(12:0)PE, and cholesterol. We find that electroformation and hydration methods result in only minor shifts (≤ 5 mole%) in lipid ratio relative to the stock solution. It was previously known that the remaining method, emulsion transfer, severely reduces the amount of cholesterol in membranes. Here, we show that the emulsion transfer method also skews the ratios of lipids in a chain-dependent manner. For example, vesicles made by emulsion transfer using only PC-lipids contain less unsaturated lipid (di(16:1)PC relative to di(16:0)PC) and less shorter-chain lipid (di(16:1)PC relative to di(18:1)PC). A separate technique, extrusion, is often used by researchers to convert giant vesicles into smaller vesicles. We find that extrusion decreases cholesterol fractions (by 5.0 ± 3.3 mol% in vesicles that originally contained ~25 mole% cholesterol). Even if all researchers were to use the same method of making vesicles, a separate question arises about whether vesicle lipid compositions vary from experiment to experiment. For the most common methods of producing GUVs (electroformation and gentle hydration), sample-to-sample variations in average lipid ratios are roughly ±2 mole%.

SIGNIFICANCE STATEMENT:

Small changes to the amounts and types of lipids in membranes can drastically affect the membrane's behavior. Unfortunately, it is unknown whether (or to what extent) different methods of making vesicles alter the ratios of lipids in membranes, even when identical stock solutions are used. This presents challenges for researchers when comparing data with colleagues who use different methods. Here, we measure ratios of lipid types in vesicle membranes produced by five methods and assess each method's reproducibility. In doing so, we provide a quantitative basis that the scientific community can use to estimate whether differences between their results can be simply attributed to differences between methods or to sample-to-sample variations.

INTRODUCTION:

Giant unilamellar vesicles (GUVs) come in many forms, from simple models of minimal membranes to complex mimics of living cells. Each application of GUVs requires that different constraints be met, such as controlling vesicle size (1–3), number of lamellae (4–6), compositional asymmetry (7–9), membrane charge (10, 11) and encapsulation of solutes (12, 13). In response, many methods have been developed to produce GUVs (14), where each method prioritizes different constraints. However, when the community uses more than one method to make GUVs, an uncomfortable question arises: do the vesicles produced by each method contain the same ratio of lipids as the stock solution from which the vesicles were made? If not, do all methods alter the intended lipid ratio in the same way, or does each method yield different ratios? These straightforward questions have a huge impact: researchers who use different methods cannot compare their results unless they know that their vesicle compositions are comparable, or, at the least, unless they know how to estimate the magnitude of the offset in lipid composition they might observe.

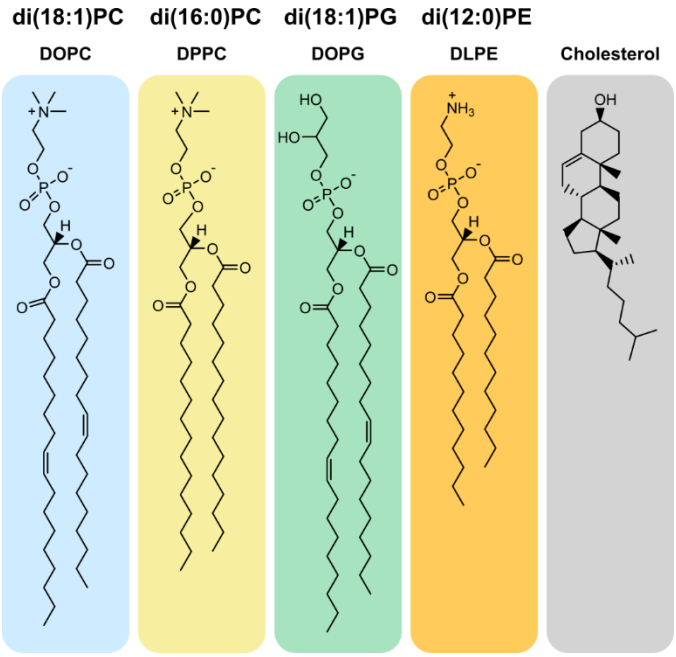

Figure 1. Structures of several lipids frequently found in GUVs. Formal names of lipids reflect the length and unsaturation of the acyl chains and the headgroup type, whereas common names reflect historical sources. For example, di(18:1)PC (commonly called DOPC) is a zwitterionic lipid with a phosphatidylcholine (PC) headgroup and two 18-carbon chains, each with one double bond, whereas di(16:0)PC is saturated, with 16 carbons in each chain. Di(18:1)PG is a charged and unsaturated lipid with a phosphatidylglycerol (PG) headgroup. Phosphatidylethanolamine (PE) headgroups, as in di(12:0)PE, are smaller than PC headgroups, so PE-lipids are typically cone-shaped. Cholesterol has a hydroxyl moiety as a headgroup and a fused, four-ring structure with an 8-carbon chain.

Concerns that different vesicle-making methods may incorporate different ratios of lipids into membranes are well-founded, especially when one of the lipids is a sterol. The solubilities of sterols in membranes of giant vesicles are sensitive to experimental conditions and to the identities of the other lipids in the membrane (15–18). Even when the mole fraction of cholesterol is below its membrane solubility limit, extrusion of vesicles may perturb the cholesterol fraction (19). Cholesterol levels are known to be especially low in vesicles made by emulsion transfer techniques (20–22). Challenges also exist in incorporating sufficient lipids with high melting temperatures (23), high charge (11, 24) or high spontaneous curvature (4) into membranes of giant vesicles.

Here, we used mass spectrometry to directly measure average mole fractions of lipids in vesicles made by multiple methods. To minimize experimental error, we produced the vesicles from a common lipid stock solution. We chose the lipids in our stock to span a broad range of characteristics (Fig. 1). They include cylindrical, zwitterionic lipids with both low and high melting temperatures (di(18:1)PC and di(16:0)PC), a charged lipid (di(18:1)PG), a cone-shaped lipid (di(12:0)PE), and a sterol (cholesterol). Each lipid is included for a different reason. PC-lipids produce stable membranes and are the most abundant lipid in mammalian cells (25–27). PG-lipids are abundant in mycobacteria (28). Their low pKa (29) and subsequent charge can increase the yield of vesicles made by gentle hydration, as does charged phosphatidylserine (PS) lipids (10). PE-lipids facilitate membrane fusion and are abundant in the inner leaflet of red cell membranes (25, 27, 30). Cholesterol, in addition to facilitating membrane fusion (31), enables large-scale, liquid-liquid phase separation in membranes (32) and constitutes a large fraction (up to ~40 mole%) of lipids in mammalian membranes (27). We mixed these lipids in a ratio likely to produce high yields of giant vesicles. Specifically, our stock solution contains high fractions of PC-lipids to stabilize GUVs and low fractions of PE-lipids to avoid inverted hexagonal phases and minimize tubule formation (25). Similarly, we use low fractions of PG-lipids to enable electroformation and low fractions of cholesterol to avoid its membrane solubility limit (15–18).

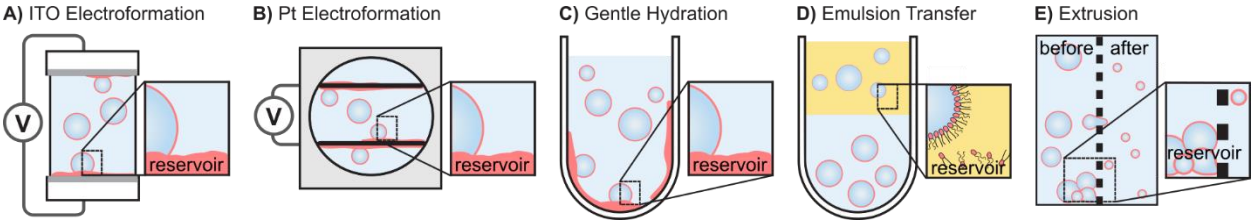

Figure 2. Methods of producing vesicles, showing reservoirs of unincorporated lipids. A) In "ITO electroformation", an alternating field is applied across a hydrated lipid film on slides coated with indium tin oxide. Afterward, a residue of lipid remains on the slide. **B)** In "Pt electroformation", an alternating field is applied across a hydrated film on platinum wires. Afterward, a residue of lipids remains on the wires. **C)** In gentle hydration, vesicles form spontaneously from a hydrated lipid film on a glass surface. Afterward, a residue of lipids remains on the glass. **D)** In emulsion transfer, lipids from an oil solution assemble at water/oil interfaces to form emulsion droplets, which then pass through a second interface to form vesicles. Afterward, a reservoir of lipids remains in the oil. **E)** In extrusion, smaller vesicles are made by passing giant vesicles through a porous filter. Afterward, a reservoir of lipids and vesicles remain on the filter. Figures are not to scale.

We chose four common techniques of producing GUVs: electroformation on slides coated with indium tin oxide (ITO), electroformation on platinum (Pt) wires, emulsion transfer, and gentle hydration (Fig. 2). We also included a common technique of converting giant vesicles into smaller vesicles: extrusion across a porous membrane filter. Each technique has advantages. Electroformation produces stable GUVs that span a wide range of sizes, frequently up to 100 µm (33). Emulsion transfer is valued for high encapsulation efficiency (34). Gentle hydration incorporates (and often requires) charged lipids in GUVs (10). Extrusion converts GUVs into vesicles of smaller and more uniform sizes. Each technique leaves a reservoir of excess lipids that were not incorporated in the vesicles. These reservoirs may not contain the same ratio of lipids as the vesicles (Fig. 2, insets).

Our use of mass spectrometry to measure average vesicle compositions complements recent advances in using Time-of-Flight Secondary Ion Mass Spectrometry (ToF-SIMS) to directly measure vesicle-to-vesicle variations in lipid compositions (35). The two techniques are synergistic. Whereas current ToF-SIMS analyses excel at measuring relative compositions in individual vesicles, the technique currently has low sample-to-sample reproducibility for vesicle populations (35). Our mass spectrometry technique does the opposite. It excels in reproducibly evaluating lipid ratios in vesicle populations and does not evaluate compositions of individual vesicles.

MATERIALS AND METHODS:

Chemicals. PC-lipids, PG-lipids, PE-lipids, and all lipid standards for mass spectrometry were obtained from Avanti Polar Lipids and used without further purification. Lipids are denoted for their headgroup (e.g., “PC”, “PG”, or “PE”), the number of carbon chains (e.g., “di” = 2), and each chain’s number of carbons and unsaturation (e.g., “18:1”). Specific lipids in our samples include dioleoyl-phosphocholine (di(18:1)PC or DOPC, T_{melt} = -18.3 ± 3.6°C (36)), dipalmitoyl-phosphocholine (di(16:0)PC or DPPC, T_{melt} = 41.3 ± 1.8°C (36)), dioleoyl-phosphoglycerol (di(18:1)PG or DOPG, T_{melt} = -18°C (37)), and dilauroyl-phosphoethanolamine (di(12:0)PE or DLPE, T_{melt} = 49.3 ± 1.7°C (38)). Lipid standards include di(15:0)PC, (16:0/18:1)PC, di(15:0)PE, di(15:0)PG, and d7-cholesterol. Cholesterol (Sigma-Aldrich) and a fluorescently labeled lipid (Texas Red DPPE, Life Technologies) were dissolved in choloroform at 10 mg/mL and 1 mg/mL, respectively. Mineral oil (light, bioreagent, 0.84 g/mL, 14.2-17.2 cSt at 40°C) was from Sigma Aldrich.

Master Stock. A master lipid stock solution was prepared for a 5-component mixture (DOPC/DPPC/DOPG/DLPE/Cholesterol with 0.8% Texas Red-DPPE) in chloroform and stored at -20°C in a vial sealed with Teflon tape and electrical tape.

Electroformation on ITO Slides. Electroformation followed standard procedures (33). Briefly, for each sample, 0.25 mg of total lipid (29 µL of master stock solution) was heated to 60°C and spread across two ITO-coated glass slides using the side of a glass Pasteur pipette. The slides were placed under vacuum for ~30 min to allow residual chloroform to evaporate. An electroformation chamber was made by sandwiching 0.3 mm thick Teflon spacers between the ITO-coated slides. The chamber was filled with 300 mM sucrose (~300 µL) and sealed with vacuum grease. The chamber was then attached to metal electrodes using stainless steel binder clips. An AC voltage of 1.0 V was applied across the electrodes at 10 Hz for 2 hr at 60°C. The temperature of 60°C is roughly 20°C above the highest lipid T_{melt} in the system.

Electroformation on Platinum wires. A chamber was adapted from previous designs (39). Briefly, a vertical hole of 15 mm diameter was cut in a 25 mm x 25 mm x 5 mm block of Teflon. Two holes of ~0.25-mm diameter were cut horizontally through the chamber, separated by 2.5 mm. Two 0.25-mm platinum wires were inserted into the two holes. Before each use, the wires and chamber were cleaned with chloroform. The bottom of the Teflon chamber was sealed with a glass cover slip, and the chamber was placed on a 60°C hot plate. Next, 5.7 µL of master stock solution was deposited in evenly spaced 0.5-µL drops on both wires. The interior of the chamber was filled with 300 mM sucrose solution, and the top was sealed with a glass cover slip. An AC voltage of 2.5 V was applied at 10 Hz for 2 hr at 60°C.

Gentle Hydration. For each sample, 0.2 – 0.8 mg of total lipid from the master stock was transferred into a glass test tube. The test tube was placed in a water bath at > 50°C while chloroform was removed from the lipid solution by a steady stream of N_2 gas to form a lipid film. To remove residual chloroform from the film, the test tube was placed under vacuum for ≥1 hr. After drying, the lipid film was rehydrated by adding 0.2 - 0.8 mL of 300 mM sucrose, so that the test tube contained 1 mL of solution for every 1 mg of lipid. The test tube was sealed with parafilm and maintained in an oven at 50°C for 24 hr. while vesicles formed.

Emulsion Transfer. The procedure was adapted from standard protocols (21, 34, 40) and was conducted at room temperature (20-25°C). A lipid film was deposited inside a test tube by drying 45.8 µL of master stock solution (0.4 mg total lipid) under a gentle stream of nitrogen gas and placing the test tube in a vacuum chamber for ≥ 30 min. The test tube and a sealed container of mineral oil were quickly transferred to a glove box (Techni-Dome 360° Glove Box Chamber) which was then purged with N_2 gas until humidity reached ≤ 25% (ThermPro Digital Indoor Thermometer). The container of mineral oil was opened only in the glove box, and 200 µL of mineral oil was added to the test tube. The test tube was sealed with Teflon, parafilm, and electrical tape, removed from the glove box, and sonicated in a water bath (CO-Z Digital Ultrasonic Cleaner Model 10A, 40 kHz) for ≥ 30 min at 50°C. The resulting lipid-in-oil solution was mixed with 20 µL of an aqueous, 300 mM sucrose solution by vigorous pipetting or by mechanical agitation to create an emulsion. Approximately 200 µL of the emulsion was layered above 300 µL of an aqueous, 300 mM glucose solution in a 1.5 mL microcentrifuge tube and then centrifuged at 9000 g for 30 min to drive dense, sucrose emulsion droplets through the oil/water interface. The supernatant was removed without disturbing the vesicle pellet until minimal solution covered the pellet. The pellet was resuspended in 600-800 µL of 300 mM glucose by gentle pipetting, using tips that had been cut to larger diameters to minimize shearing.

Vesicle Sedimentation and Storage. For vesicles made by electroformation and gentle hydration, vesicles were separated from lipid aggregates by sedimenting vesicles in an osmotically matched glucose solution as in Fig. S1. Briefly, 200 µL of vesicle solution was added on top of 800 µL of glucose solution in a 13x1000 glass test tube (Fisher Scientific). Vesicles sank to the bottom of the tube for 10 min. Then 150 µL of vesicle solution was transferred from the bottom of the tube to a microcentrifuge tube. For emulsion transfer, vesicles were sedimented after resuspension in 600-800 µL of a glucose solution. For all methods, separated vesicle samples were stored at -20°C in parafilm-sealed 1.5 mL microcentrifuge tubes.

Vesicle Imaging. To verify that the four methods above produced giant vesicles, vesicle solutions were imaged between glass slides on a Nikon Eclipse ME600L upright epifluorescence microscope using a Hamamatsu C13440 camera at room temperature (25°C).

Extrusion. Vesicle solutions were prepared by gentle hydration, and then sedimented to remove lipid aggregates. The sedimented vesicle solution was split into two samples of equal volume. The first sample was reserved for “Before” extrusion measurements and the second sample was extruded to obtain an “After” measurement. To minimize the loss of solution due to dead volume of the miniextruder (Avanti Polar Lipids), the filter supports and 0.1 µm polycarbonate filter were prewet by passing 1 mL of a sucrose solution through them prior to loading the sample. The complete extruder assembly (the heat block, the syringe with the vesicle solution, and the empty syringe) was maintained at 50 °C for 30 min before extrusion. Finally, the vesicle solution was passed through the filter 9 times and collected for analysis.

HILIC-IM-MS Analysis of Phospholipids. Internal lipid standards were added to samples prior to lipid extraction to account for lipid loss during extraction and to aid in relative quantitation for each lipid class. Total lipids from aliquots of each sample were extracted by the method of Bligh and Dyer (41). Extracts were dried in a vacuum concentrator and reconstituted in 2:1 acetonitrile-methanol. Lipid analysis was conducted using hydrophilic interaction liquid chromatography (HILIC) coupled with ion mobility-mass spectrometry (IM-MS) in positive electrospray ionization mode (Waters Synapt XS HDMS; Waters Corp., Milford, MA). Chromatographic separations were carried out using a Phenomenex Kinetex HILIC column (50 x 2.1 mm, 1.7 µm) with 95% acetonitrile/5% water/5 mM ammonium acetate as mobile phase A and 50% acetonitrile/50% water/5 mM ammonium acetate as mobile phase B (Waters Acquity FTN UPLC; Waters Corp.). Collisional cross-section calibration and IM-MS analysis were conducted as described previously (42–44). Data alignment and peak detection were performed in Progenesis QI (Nonlinear Dynamics; Waters Corp.). Retention time calibration and lipid identification were calculated with the LiPydomics Python package (45). Lipid abundances were normalized to their internal standards.

For the five methods tested, the lipid components were normalized to the following internal standards: di(16:0)PC and di(18:1)PC to di(15:0)PC, di(12:0)PE to di(15:0)PE, and di(18:1)PG to di(15:0)PG. For the two-component emulsion transfer measurements, the master stock solution included mass spectrometry standards for saturated and unsaturated lipids (di(15:0)PC and (16:0)(18:1)PC, respectively).

UHPLC-MS/MS Analysis of Cholesterol. An internal standard d_7-cholesterol was added with lipid standards to samples prior to extraction. The same extracts were used for analysis of phospholipids and cholesterol. Extracts were prepared as described in the previous section and analyzed through ultra-high performance liquid chromatography-tandem mass spectrometry (UHPLC-MS/MS) using atmospheric pressure chemical ionization (Sciex QTRAP 6500; SCIEX, Framingham, MA or Waters Xevo TQ-XS; Waters Corp.) (46). Reversed-phase chromatography separations were carried out using a Phenomenex Kinetex C18 column (100 x 2.1 mm, 1.7 µm) with a 90% methanol/10% water/0.1% formic acid mobile phase. Quantitation methods and peak integration were performed using Analyst software (SCIEX Analyst 5.1; SCIEX) or MassLynx and TargetLynx software (Waters Corp.). Concentrations of cholesterol were obtained using peak ratios relative to d_7-cholesterol (46).

Analysis and Plotting. The lipid abundances are the raw values obtained from the mass spectrometry measurements. To calculate lipid composition as mole percentages, the abundance of each lipid (normalized to a lipid standard) was divided by the total lipid abundance for each sample (Table S5). The mean percentage of each lipid type and the standard deviation were calculated for three independent samples. Ternary plots were generated using the open-source Python library, python-ternary (https://github.com/marcharper/python-ternary).

RESULTS AND DISCUSSION

Our experiments answer four types of questions: 1) Do all methods produce giant vesicles with sufficient yield? 2) How do the ratios of lipids in vesicles produced by each method differ from ratios in vesicles produced by the other methods, 3) How do those ratios differ from the stock solution, and 4) How reproducible is each method?

All methods produce giant unilamellar vesicles.

As expected, electroformation on either ITO slides or platinum wires typically produces high yields of unilamellar vesicles (Fig. S2 and Fig. S3). Electroformation on platinum wires form smaller vesicles than electroformation on ITO slides; however, the size and physical separation of the wires can impact the size of the GUVs formed. Vesicles made by gentle hydration consistently have more lamellae or nested vesicles (Fig. S4), and vesicles made by emulsion transfer consistently have defects of lipid aggregates or nested vesicles (Fig. S5). Vesicles extruded through 100 nm membrane filters are too small to be resolved (Fig. S6).

Vesicles made by electroformation and gentle hydration exhibit liquid-liquid phase separation of their membranes, consistent with the tendency for membranes to demix when they contain mixtures of high-T_{melt} lipids, low-T_{melt} lipids, and cholesterol (23). In contrast, the vesicles prepared by emulsion transfer did not exhibit liquid-liquid phase separation at room temperature, indicating that the lipid composition of emulsion transfer vesicles differed from the lipid composition of the other vesicles (Fig. S5).

Electroformation and gentle hydration create vesicles with minor offsets in lipid ratios.

Our central result is that three methods of producing giant vesicles (electroformation on ITO slides, electroformation on platinum wires, and gentle hydration) result in similar percentages of lipids in the membranes. Moreover, these percentages are similar to that of the master stock solution. These similarities are shown in the first four stacked bars in Fig. 3A.

Another way to visualize the minor differences in lipid ratios between the three methods is to zoom into a region of the pseudo-ternary diagram in Fig. 3B. Lipid compositions of vesicles made by the two electroformation methods (triangles and circles) and the gentle hydration method (squares) cluster around the master stock solution (star). Fig. 3B shows that electroforming vesicles on ITO slides and on platinum wires shifts lipid mole ratios from the master stock solution by roughly 3.5 mole% and 1.5 mole%, respectively. Similarly, gentle hydration of vesicles shifts lipid mole ratios by roughly 4 mole%, in the direction of increasing cholesterol. The data in Fig. 3 also show that reproducibility of the electroformation and hydration methods is high, based on the close clustering of data from three independent experiments. The range of sample-to-sample lipid ratios for each method is within ±2 mole%.

Our result that electroformation and gentle hydration do not produce vesicles with wildly different mole fractions of cholesterol is consistent with reports that the maximum amount of cholesterol that can be incorporated into membranes is roughly equivalent for vesicles made by electroformation (between 65 and 70 mole% (18), gentle hydration (61 mole% (47) or ≤63 mole% (15), and a third method, rapid solvent exchange (66 ± 1 mole% (15)). Recent ToF-SIMS data disagree with these results, but have low reproducibility: in two independent experiments, the amount of cholesterol in GUVs made by electroformation was either roughly one-quarter or two thirds of that in GUVs made by gentle hydration (35).

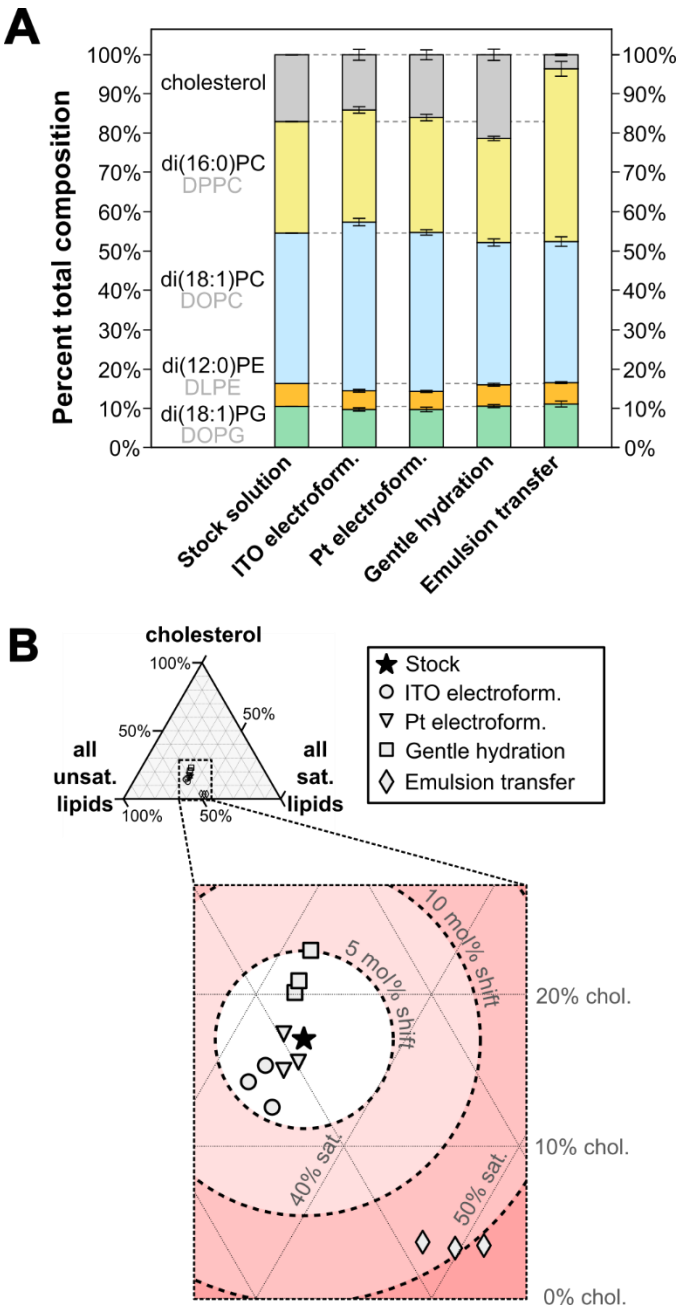

Figure 3. Lipid percentages in 5-component vesicles produced by different methods. **A)** Percent of each lipid component in the master stock solution and in the three independent vesicle solutions of each technique made from the master stock solution. Values are averages, and error bars above each section of the bar chart are standard deviations of three independent experiments. Full data appear in Tables S1, S5, and S6. **B)** Lipid percentages for the three independent solutions of each technique plotted on a pseudo-ternary diagram, where the three vertices represent cholesterol, the sum of the saturated lipids (di(16:0)PC and di(12:0)PE), and the sum of the unsaturated lipids (di(18:1)PC and di(18:1)PG).

Shifts in lipid compositions in Figure 3 are largely due to different mole fractions of cholesterol in vesicles with respect to the master stock solution. In contrast, only small shifts of ~1 mole% are seen in PE-lipid and PG-lipids (Fig. S7). These shifts are the same magnitude as sample-to-sample differences of independent experiments. The small shift in di(12:0)PE seems surprising in light of previous studies using lipid mixtures extracted from rabbit sarcoplasmic reticulum: PE-lipids were grossly over-represented in the lipids left behind on a glass substrate (4). The particular lipid we use, di(12:0)PE, may integrate better into vesicles than other PE lipids because it is in a liquid, lamellar phase (rather than a gel phase or an inverted hexagonal phase). In contrast, the small shift in the charged PG-lipid is not as surprising, at least for gentle hydration. Blosser et al. found no statistically significant shift in the mole fraction of diphytanoylPG lipids with respect to a stock solution for vesicles that were made by gentle hydration (11). Similarly, Angelova found no significant difference in the mole fractions of charged (PS-lipids) and uncharged lipids (PC-lipids) between a vesicle solution made by gentle hydration and a lipid film left behind on a glass surface (4).

How will the minor shifts in lipid ratios we observe in Fig. 3 impact how the biophysics community interprets data from GUVs? It depends on how experiments are designed. Broad conclusions derived from experiments that increment stock lipid compositions by ~5 mole% will likely apply equally well to vesicles electroformed on ITO slides or on platinum electrodes, and may slightly differ when applied to vesicles made by gentle hydration. In contrast, detailed conclusions that depend on incrementing lipid compositions by only ~1 mole% will likely apply only to vesicles made by a single method and will likely be affected by sample-to-sample differences. More detailed conclusions are difficult to extract from the data in Fig. 3 because only the percentages of the lipids (rather than their absolute values) are relevant. For example, an increase in the ratio of cholesterol to phospholipids could be due to an absolute increase in cholesterol, an absolute decrease in phospholipids, or both.

Emulsion transfer results in too little cholesterol in vesicles.
Emulsion transfer forms vesicles with less cholesterol. Unlike the electroformation and gentle hydration methods, the emulsion transfer method creates large shifts in lipid compositions of vesicles (Fig. 3). When compared to the master stock solution, the emulsion phase transfer method incorporated only ~20% of the expected amount of cholesterol. This result is consistent with previous reports of low cholesterol in vesicle membranes made by emulsion techniques such as cDICE (<1% of the expected cholesterol (20), double-layer cDICE (25-35% of the expected cholesterol (22)), emulsion phase transfer (28-50% of the expected cholesterol (21)), and droplet shooting size-filtration (33-50% of the expected cholesterol (48), as discussed in (20)). The problem likely arises because cholesterol lacks a large polar headgroup to drive it out of bulk oil, toward an interface with water. The problem can be mitigated, but not eliminated, by switching from heavy (20) to light mineral oil as we and others did (21) .

Too much saturated and long-chain PC-lipids in vesicles made by emulsion transfer.
We were surprised to find that the emulsion transfer method also vastly skews the ratio of the PC-lipids; di(16:0)PC is over-represented by a factor of ~1.5 in the vesicles compared to the master stock solution (Fig. 3). The effect is so large that nearly all loss of cholesterol in emulsion transfer vesicles appears to be counteracted by a gain in di(16:0)PC. To our knowledge, shifts in phospholipid compositions have not previously been measured in emulsion transfer vesicles.

Two structural characteristics of di(16:0)PC could have caused it to be over-represented relative to di(18:1)PC in vesicles made by emulsion transfer: chain length and saturation. To determine whether each of these characteristics is salient on its own, we designed two additional experiments. In the first experiment, we made a 50:50 stock solution of lipids that differ only in their degree of unsaturation: di(16:0)PC and di(16:1)PC. We found that vesicles made by emulsion phase transfer from this stock solution contained significantly more saturated lipid, in a ratio of 60:40 (Fig. 4A). The stock solution did not contain cholesterol, so the over-representation of the saturated lipid is not due to known, favorable interactions between cholesterol and saturated lipids (49). In the second experiment, we made a 50:50 stock solution of lipids that differ only in their chain length: di(16:1)PC and di(18:1)PC. We found that vesicles made by emulsion phase transfer from this stock solution contained 3-10 mol% more of the longer-chain lipid, but with lower reproducibility (Fig. 4B).

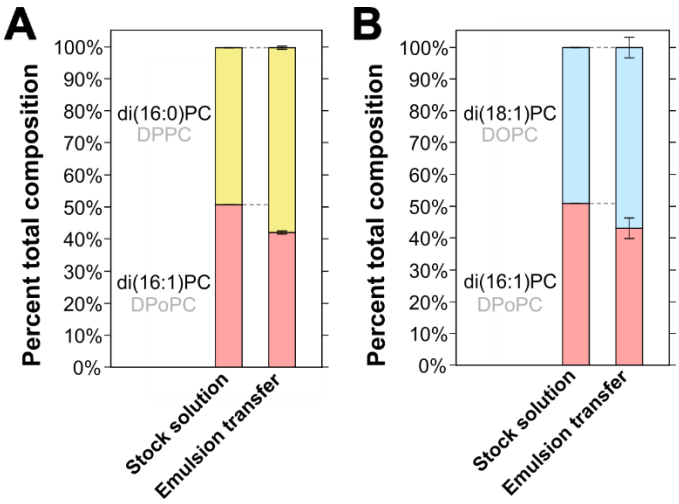

Figure 4. Emulsion phase transfer incorporates more saturated and long-chain lipids into vesicles A) Ratio of lipids in vesicles made from a stock, 50:50 mixture of two PC-lipids with chain lengths of 16 carbons, one saturated and one unsaturated. **B)** Lipid composition of vesicles made from a stock solution containing two unsaturated PC lipids, one with a chain length of 18 carbons and one with a chain length of 16 carbons. In both panels, values are averages, and error bars above each section of the bar chart are standard deviations of three independent experiments. Full data appear in Tables S2 and S3.

Extrusion of vesicles results in lower cholesterol fractions.

Some powerful techniques of assessing membrane phase behavior use giant vesicles whereas others (e.g., electron microscopy and neutron scattering (50–52)) require ~100 nm vesicles, produced by extruding vesicles through polycarbonate filters. Here, we conducted a new series of experiments to compare ratios of lipids in solutions of giant vesicles generated by gentle hydration with ratios from the same solutions after extrusion (Fig. S6).

We find decreases in cholesterol due to extrusion (Fig. 5). In terms of absolute numbers, these shifts are not huge, a decrease of 5.0 ± 3.3 mol% cholesterol, where the uncertainty is the standard deviation for three independent experiments. In terms of the total percent of cholesterol, the shifts are significant, roughly 1/5 of cholesterol is lost upon extrusion of vesicles made by gentle hydration. This value is in between reports of no loss of cholesterol from some membranes (specifically, for binary membranes of 33% cholesterol with di(18:1)PC or di(14:0)PC or for ternary mixtures of 2:1:3 PC-lipids/eggPC/cholesterol) and a loss of ~1/3 to ~1/2 of cholesterol from other membranes (namely for binary membranes of 33% cholesterol with 16:0/18:1PC, di(16:0)PC, or di(20:4)PC) (19). In other words, no clear trend has been uncovered to explain how lipid unsaturation affects the loss of cholesterol from vesicles upon extrusion.

We find that the decrease in cholesterol upon extrusion is offset by smaller increases in PC-lipids (1.4 ± 0.7 mol% for di(16:0)PC, and 1.5 ± 0.8 mol% for di(18:1)PC, respectively). Shifts in PE- and PG-lipids are insignificant (0.4 ± 0.9 mol% for di(12:0)PE and 2.5 ± 3.4 mol% for di(18:1)PG). As before, the main conclusion is that experiments that report results at high precision (e.g., 1 mole%) will be sensitive to how vesicles are made and to sample-to-sample differences.

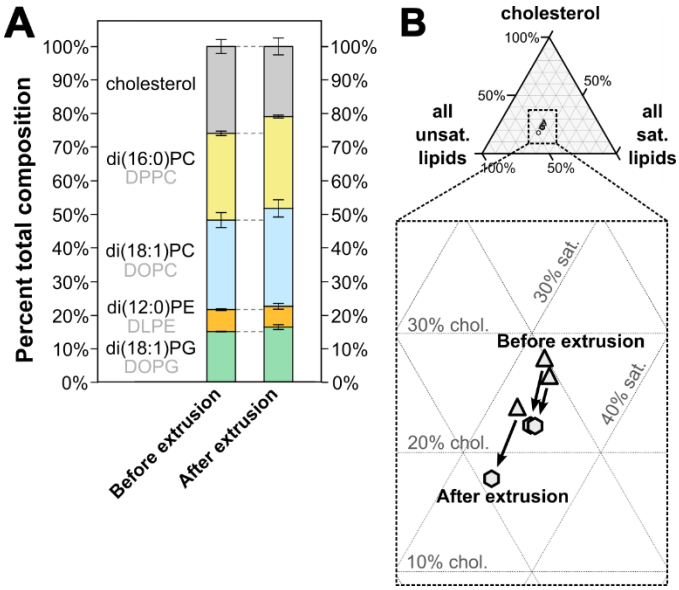

Figure 5. Extrusion of giant vesicles decreases their cholesterol content. A) Percentage of all five lipids in vesicles made via gentle hydration, before and after extrusion through a 0.1 µM filter. Values are averages, and error bars above each section of the bar chart are standard deviations of three independent experiments. **B)** Mole fractions of each experiment plotted on a pseudo-ternary diagram, before and after extrusion. The three vertices correspond to cholesterol, the sum of the saturated lipids (di(16:0)PC and di(12:0)PE), and the sum of the unsaturated lipids (di(18:1)PC and di(18:1)PG). Full data appear in Tables S5 and S6. These gentle hydration samples were prepared and measured separately from samples comparing the four other methods.

Caveats

In the sections above, we tested whether several methods of making vesicles skew the ratio of lipids in membranes. Many unexplored variations on each method exist. For example, we made vesicles by gentle hydration in water rather than in salt solutions, and the vesicles formed on a glass surface rather than on polymer-coated substrates (53, 54) or on tracing paper (55). Similarly, we converted giant vesicles into smaller vesicles by extruding them rather than by freeze/thaw cycles or sonication.

Similar caveats apply to the choice of master stock solution. Many lipid mixtures are equally relevant and may produce different shifts in lipid ratios. Whenever lipid stocks contain small fractions of some lipids (like the PE-and PG-lipids in our sample), small shifts in their mole fractions will be observed, even if the percent change is high. Although we found small shifts in all lipid fractions for most methods, it is worth bearing in mind that small shifts can result in big changes, especially in lipid phase behavior. If a membrane lies near a phase boundary, a tiny shift in its lipid composition can lead a previously uniform membrane to demix into coexisting phases, or a liquid membrane to turn into a gel phase. For researchers who are comparing vesicles made by different methods, a best practice is to choose a ratio of lipids that lies in the middle of whatever phase region is desired.

CONCLUSIONS:

In summary, electroformation and gentle hydration, the most common methods of producing GUVs, result in minor shifts (≤5 mole%) in the lipid ratio relative to a stock solution and minor (±2 mole%) sample-to-sample variations for independent experiments. Researchers will find the magnitudes of these shifts to be either comfortingly small or alarmingly large, depending on how they design their experiments. For example, experiments that report concentrations incremented by only ~1 mole% will be highly sensitive to the vesicle-making method and to sample-to-sample differences. An additional method (emulsion transfer) results in large shifts. Although it was previously known that vesicles made by emulsion transfer contain much less cholesterol than the stock solutions from which they are made, we found the surprising result that emulsion transfer vesicles also contain less unsaturated lipid and less shorter-chain lipid. Extrusion of vesicles can further decrease a membrane's cholesterol content.

AUTHOR CONTRIBUTIONS:

All authors designed research and protocols. HMJW, KJW, GJG, ELP, and AL performed research and analyzed data. SLK, HMJW, KJW, and GJG wrote the manuscript. All authors edited the manuscript.

ACKNOWLEDGEMENTS:

We thank the staff at the UW Statistical Consulting Services for their expertise. HMJW was supported by the National Institute of General Medical Sciences of the National Institutes of Health under Award Number T32GM008268. This research was supported by National Science Foundation grant MCB-1925731 and MCB-2325819 to SLK and by National Institutes of Health grant R01HD092659 and R01 AI136979 to LX.

DECLARATION OF INTERESTS:

The authors declare no competing interests.

REFERENCES:

1. Olson, F., C.A. Hunt, F.C. Szoka, W.J. Vail, and D. Papahadjopoulos. 1979. Preparation of liposomes of defined size distribution by extrusion through polycarbonate membranes. *BBA - Biomembr.* 557:9–23.

2. Sugiura, S., T. Kuroiwa, T. Kagota, M. Nakajima, S. Sato, S. Mukataka, P. Walde, and S. Ichikawa. 2008. Novel Method for Obtaining Homogeneous Giant Vesicles from a Monodisperse Water-in-Oil Emulsion Prepared with a Microfluidic Device. *Langmuir*. 24:4581–4588.

3. Zhu, T.F., and J.W. Szostak. 2009. Preparation of Large Monodisperse Vesicles. *PLoS ONE*. 4:e5009.

4. Angelova, M.I. (1988). Lipid Swelling and Liposome Formation in Electric Fields. PhD thesis. Bulgarian Academy of Sciences.

5. Ghellab, S.E., Q. Li, T. Fuhs, H. Bi, and X. Han. 2017. Electroformation of double vesicles using an amplitude modulated electric field. *Colloids Surf. B Biointerfaces*. 160:697–703.

6. Ip, T., Q. Li, N. Brooks, and Y. Elani. 2021. Manufacture of Multilayered Artificial Cell Membranes through Sequential Bilayer Deposition on Emulsion Templates. *ChemBioChem*. 22:2275–2281.

7. Pautot, S., B.J. Frisken, and D.A. Weitz. 2003. Engineering asymmetric vesicles. *Proc. Natl. Acad. Sci.* 100:10718–10721.

8. Elani, Y., S. Purushothaman, P.J. Booth, J.M. Seddon, N.J. Brooks, R.V. Law, and O. Ces. 2015. Measurements of the effect of membrane asymmetry on the mechanical properties of lipid bilayers. *Chem. Commun.* 51:6976–6979.

9. Doktorova, M., F.A. Heberle, B. Eicher, R.F. Standaert, J. Katsaras, E. London, G. Pabst, and D. Marquardt. 2018. Preparation of asymmetric phospholipid vesicles: The next generation of cell membrane models. *Nat. Protoc.* 13:2086–2101.

10. Akashi, K., H. Miyata, H. Itoh, and K. Kinosita. 1996. Preparation of giant liposomes in physiological conditions and their characterization under an optical microscope. *Biophys. J.* 71:3242–3250.

11. Blosser, M.C., J.B. Starr, C.W. Turtle, J. Ashcraft, and S.L. Keller. 2013. Minimal Effect of Lipid Charge on Membrane Miscibility Phase Behavior in Three Ternary Systems. *Biophys. J.* 104:2629–2638.

12. Dominak, L.M., and C.D. Keating. 2007. Polymer Encapsulation within Giant Lipid Vesicles. *Langmuir*. 23:7148–7154.

13. Abkarian, M., E. Loiseau, and G. Massiera. 2011. Continuous droplet interface crossing encapsulation (cDICE) for high throughput monodisperse vesicle design. *Soft Matter*. 7:4610–4614.

14. Dimova, R., and C. Marques. 2019. The Giant Vesicle Book. CRC Press, Boca Raton.

15. Huang, J., J.T. Buboltz, and G.W. Feigenson. 1999. Maximum solubility of cholesterol in phosphatidylcholine and phosphatidylethanolamine bilayers. *BBA - Biomembr.* 1417:89–100.

16. Epand, R.M., D.W. Hughes, B.G. Sayer, N. Borochov, D. Bach, and E. Wachtel. 2003. Novel properties of cholesterol-dioleoylphosphatidylcholine mixtures. *Biochim. Biophys. Acta*. 1616:196–208.

17. Shaikh, S.R., V. Cherezov, M. Caffrey, S.P. Soni, D. LoCascio, W. Stillwell, and S.R. Wassall. 2006. Molecular Organization of Cholesterol in Unsaturated Phosphatidylethanolamines: X-ray Diffraction and Solid State 2H NMR Reveal Differences with Phosphatidylcholines. *J. Am. Chem. Soc.* 128:5375–5383.

18. Stevens, M.M., A.R. Honerkamp-Smith, and S.L. Keller. 2010. Solubility Limits of Cholesterol, Lanosterol, Ergosterol, Stigmasterol, and β-Sitosterol in Electroformed Lipid Vesicles. *Soft Matter*. 6:5882–5890.

19. Ibarguren, M., A. Alonso, B.G. Tenchov, and F.M. Goñi. 2010. Quantitation of cholesterol incorporation into extruded lipid bilayers. *BBA - Biomembr.* 1798:1735–1738.

20. Blosser, M.C., B.G. Horst, and S.L. Keller. 2016. cDICE method produces giant lipid vesicles under physiological conditions of charged lipids and ionic solutions. *Soft Matter*. 12:7364–7371.

21. Karamdad, K., J. W. Hindley, G. Bolognesi, M. S. Friddin, R. V. Law, N. J. Brooks, O. Ces, and Y. Elani. 2018. Engineering thermoresponsive phase separated vesicles formed via emulsion phase transfer as a content-release platform. *Chem. Sci.* 9:4851–4858.

22. Dürre, K., and A. R. Bausch. 2019. Formation of phase separated vesicles by double layer cDICE. *Soft Matter*. 15:9676–9681.

23. Veatch, S.L., and S.L. Keller. 2005. Seeing spots: Complex phase behavior in simple membranes. *BBA - Mol. Cell Res.* 1746:172–185.

24. Gambhir, A., G. Hangyás-Mihályné, I. Zaitseva, D.S. Cafiso, J. Wang, D. Murray, S.N. Pentyala, S.O. Smith, and S. McLaughlin. 2004. Electrostatic Sequestration of PIP2 on Phospholipid Membranes by Basic/Aromatic Regions of Proteins. *Biophys. J.* 86:2188–2207.

25. Cullis, P.R., M.J. Hope, and C.P.S. Tilcock. 1986. Lipid polymorphism and the roles of lipids in membranes. *Chem. Phys. Lipids*. 40:127–144.

26. van der Veen, J.N., J.P. Kennelly, S. Wan, J.E. Vance, D.E. Vance, and R.L. Jacobs. 2017. The critical role of phosphatidylcholine and phosphatidylethanolamine metabolism in health and disease. *BBA - Biomembr.* 1859:1558–1572.

27. Lorent, J.H., K.R. Levental, L. Ganesan, G. Rivera-Longsworth, E. Sezgin, M. Doktorova, E. Lyman, and I. Levental. 2020. Plasma membranes are asymmetric in lipid unsaturation, packing and protein shape. *Nat. Chem. Biol.* 16:644–652.

28. Brennan, P.J., and H. Nikaido. 1995. The Envelope of Mycobacteria. *Annu. Rev. Biochem.* 64:29–63.

29. Marsh, D. 2013. Handbook of Lipid Bilayers. 2nd ed. CRC Press, Boca Raton.

30. Verkleij, A.J., R.F.A. Zwaal, B. Roelofsen, P. Comfurius, D. Kastelijn, and L.L.M. van Deenen. 1973. The asymmetric distribution of phospholipids in the human red cell membrane. A combined study using phospholipases and freeze-etch electron microscopy. *BBA - Biomembr.* 323:178–193.

31. Yang, S.-T., A.J.B. Kreutzberger, J. Lee, V. Kiessling, and L.K. Tamm. 2016. The role of cholesterol in membrane fusion. *Chem. Phys. Lipids*. 199:136–143.

32. Dietrich, C., L.A. Bagatolli, Z.N. Volovyk, N.L. Thompson, M. Levi, K. Jacobson, and E. Gratton. 2001. Lipid Rafts Reconstituted in Model Membranes. *Biophys. J.* 80:1417–1428.

33. Veatch, S.L. 2007. Electro-formation and fluorescence microscopy of giant vesicles with coexisting liquid phases. *Methods Mol Biol*. 398:59–72.

34. Pautot, S., B.J. Frisken, and D.A. Weitz. 2003. Production of Unilamellar Vesicles Using an Inverted Emulsion. *Langmuir*. 19:2870–2879.

35. Grusky, D.S., A. Bhattacharya, and S.G. Boxer. 2023. Secondary Ion Mass Spectrometry of Single Giant Unilamellar Vesicles Reveals Compositional Variability. *J. Am. Chem. Soc.* 145:27521–27530.

36. Koynova, R., and M. Caffrey. 1998. Phases and phase transitions of the phosphatidylcholines. *BBA - Rev. Biomembr.* 1376:91–145.

37. Findlay, E.J., and P.G. Barton. 1978. Phase behavior of synthetic phosphatidylglycerols and binary mixtures with phosphatidylcholines in the presence and absence of calcium ions. *Biochemistry*. 17:2400–2405.

38. Koynova, R., and M. Caffrey. 1994. Phases and phase transitions of the hydrated phosphatidylethanolamines. *Chem. Phys. Lipids*. 69:1–34.

39. Witkowska, A., L. Jablonski, and R. Jahn. 2018. A convenient protocol for generating giant unilamellar vesicles containing SNARE proteins using electroformation. *Sci. Rep.* 8:9422.

40. Moga, A., N. Yandrapalli, R. Dimova, and T. Robinson. 2019. Optimization of the Inverted Emulsion Method for High-Yield Production of Biomimetic Giant Unilamellar Vesicles. *ChemBioChem*. 20:2674–2682.

41. Bligh, E.G., and W.J. Dyer. 1959. A rapid method of total lipid extraction and purification. *Can. J. Biochem. Physiol.* 37:911–917.

42. Hines, K.M., J.C. May, J.A. McLean, and L. Xu. 2016. Evaluation of Collision Cross Section Calibrants for Structural Analysis of Lipids by Traveling Wave Ion Mobility-Mass Spectrometry. *Anal. Chem.* 88:7329–7336.

43. Hines, K.M., J. Herron, and L. Xu. 2017. Assessment of altered lipid homeostasis by HILIC-ion mobility-mass spectrometry-based lipidomics. *J. Lipid Res.* 58:809–819.

44. Li, A., K.M. Hines, and L. Xu. 2020. Lipidomics by HILIC-Ion Mobility-Mass Spectrometry. *Methods Mol. Biol. Clifton NJ*. 2084:119–132.

45. Ross, D.H., J.H. Cho, R. Zhang, K.M. Hines, and L. Xu. 2020. LiPydomics: A Python Package for Comprehensive Prediction of Lipid Collision Cross Sections and Retention Times and Analysis of Ion Mobility-Mass Spectrometry-Based Lipidomics Data. *Anal. Chem.* 92:14967–14975.

46. Herron, J., K.M. Hines, and L. Xu. 2018. Assessment of altered cholesterol homeostasis by xenobiotics using ultra-high performance liquid chromatography-tandem mass spectrometry. *Curr. Protoc. Toxicol.* 78:e65.

47. Garg, S., F. Castro-Roman, L. Porcar, P. Butler, P.J. Bautista, N. Krzyzanowski, and U. Perez-Salas. 2014. Cholesterol solubility limit in lipid membranes probed by small angle neutron scattering and MD simulations. *Soft Matter*. 10:9313–9317.

48. Morita, M., H. Onoe, M. Yanagisawa, H. Ito, M. Ichikawa, K. Fujiwara, H. Saito, and M. Takinoue. 2015. Droplet-Shooting and Size-Filtration (DSSF) Method for Synthesis of Cell-Sized Liposomes with Controlled Lipid Compositions. *ChemBioChem*. 16:2029–2035.

49. Shaw, T.R., K.C. Wisser, T.A. Schaffner, A.D. Gaffney, B.B. Machta, and S.L. Veatch. 2023. Chemical potential measurements constrain models of cholesterol-phosphatidylcholine interactions. *Biophys. J.* 122:1105–1117.

50. Cornell, C.E., A. Mileant, N. Thakkar, K.K. Lee, and S.L. Keller. 2020. Direct imaging of liquid domains in membranes by cryo-electron tomography. *Proc. Natl. Acad. Sci.* 117:19713–19719.

51. Heberle, F.A., M. Doktorova, H.L. Scott, A.D. Skinkle, M.N. Waxham, and I. Levental. 2020. Direct label-free imaging of nanodomains in biomimetic and biological membranes by cryogenic electron microscopy. *Proc. Natl. Acad. Sci.* 117:19943–19952.

52. Heberle, F.A., M. Doktorova, S.L. Goh, R.F. Standaert, J. Katsaras, and G.W. Feigenson. 2013. Hybrid and Nonhybrid Lipids Exert Common Effects on Membrane Raft Size and Morphology. *J. Am. Chem. Soc.* 135:14932–14935.

53. Horger, K.S., D.J. Estes, R. Capone, and M. Mayer. 2009. Films of Agarose Enable Rapid Formation of Giant Liposomes in Solutions of Physiologic Ionic Strength. *J. Am. Chem. Soc.* 131:1810–1819.

54. Weinberger, A., F.-C. Tsai, G.H. Koenderink, T.F. Schmidt, R. Itri, W. Meier, T. Schmatko, A. Schröder, and C. Marques. 2013. Gel-Assisted Formation of Giant Unilamellar Vesicles. *Biophys. J.* 105:154–164.

55. Pazzi, J., and A.B. Subramaniam. 2020. Nanoscale Curvature Promotes High Yield Spontaneous Formation of Cell-Mimetic Giant Vesicles on Nanocellulose Paper. *ACS Appl. Mater. Interfaces*. 12:56549–56561.

Supporting Material for:

Common methods of making giant vesicles (except emulsion techniques) capture intended lipid ratios

Heidi M.J. Weakly, Kent J. Wilson, Gunnar J. Goetz, Emily L. Pruitt, Amy Li,
Libin Xu and Sarah L. Keller

This file includes:

Figures S1-S7
Data Tables S1-S10

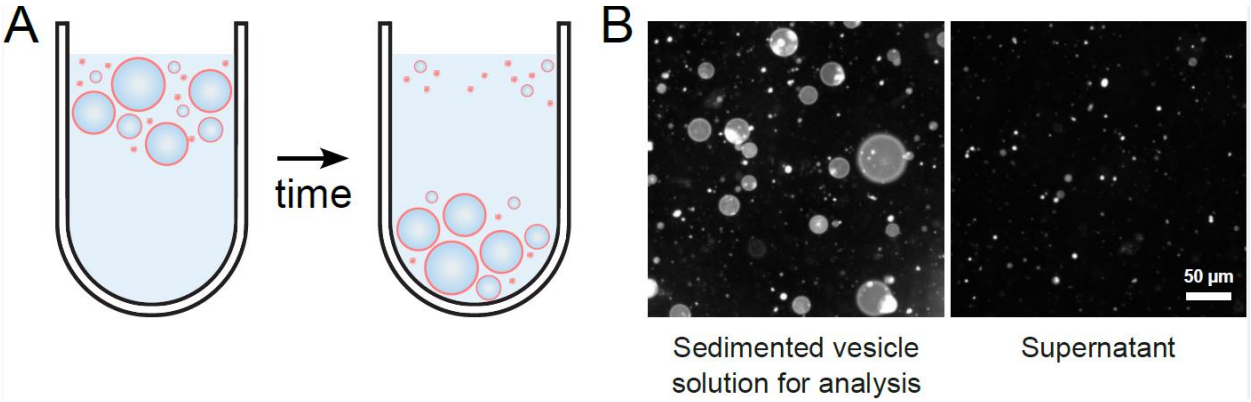

Figure S1. Sedimenting vesicles removes some lipid aggregates. A) Vesicles filled with a dense sucrose solution sink in an osmotically matched glucose solution. **B)** After sinking, large vesicles are observed only in the sedimented solution, and not in the supernatant. The vesicles in these images were made by emulsion phase transfer. The density of giant vesicles in the supernatant is representative for all techniques.

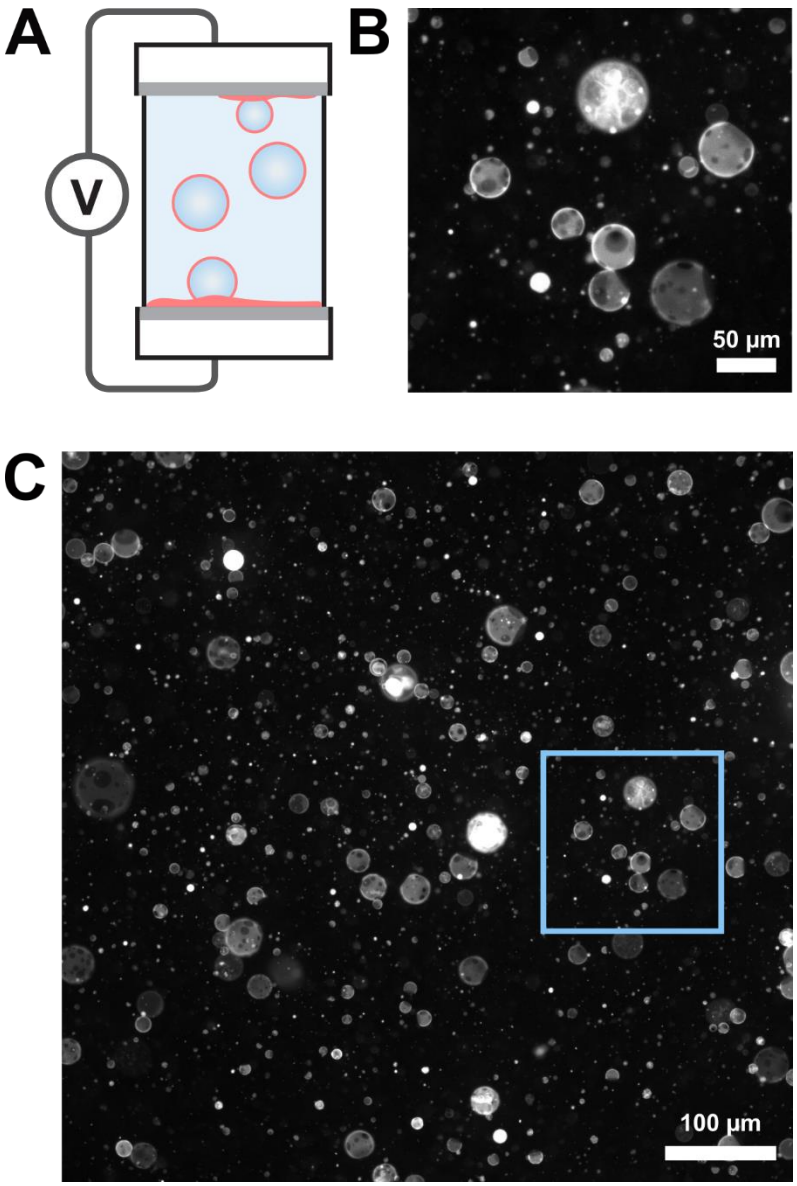

Figure S2. Representative fluorescence micrographs of vesicles made by electroformation on ITO-coated slides. A) Schematic of ITO electroformation. **B)** Close-up of vesicles in the blue box in panel C. **C)** Full field of view of vesicles produced by electroformation on ITO slides. As expected, ITO electroformation produces the highest yield of giant, unilamellar vesicles (GUVs) of the four methods tested for producing vesicles. Some multilamellar vesicles, nested vesicles (large vesicles filled with multiple small vesicles) and some bright, lipid aggregates are also produced.

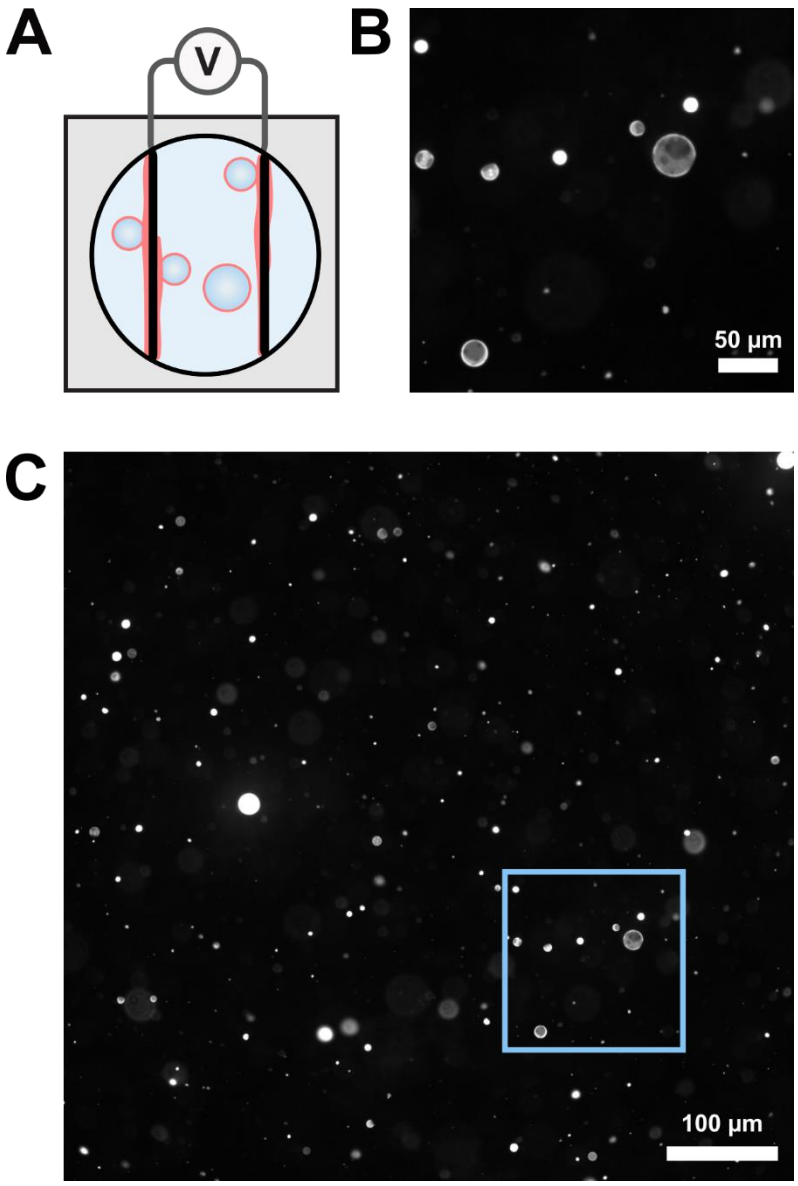

Figure S3. Representative fluorescence micrographs of vesicles made by electroformation on platinum wires. A) Schematic of Pt electroformation. **B)** Close-up of vesicles in the blue box in panel C. **C)** Full field of view of vesicles produced by electroformation on Pt wires. The volume of stock solution used is low relative to the other methods and therefore produces a lower yield of vesicles at the same stock concentration.

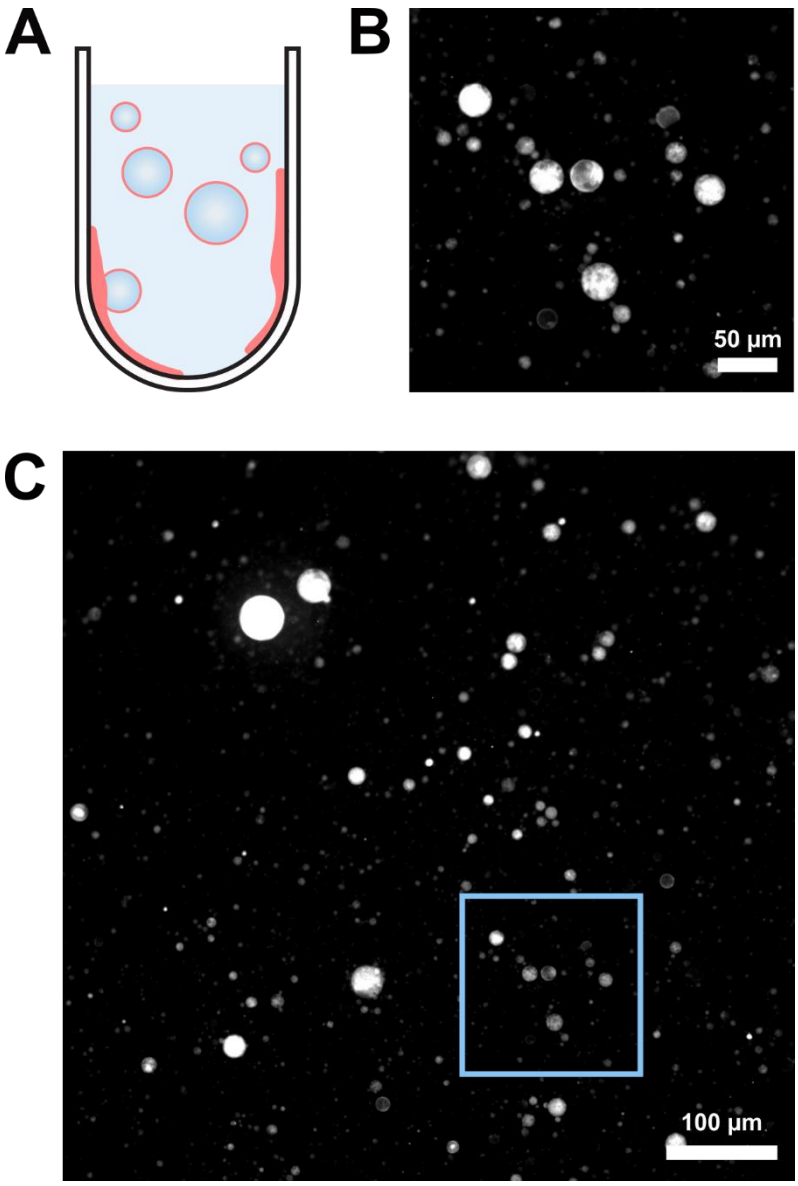

Figure S4. Representative fluorescence micrographs of vesicles made by gentle hydration for 24 hrs. A) Schematic of gentle hydration. **B)** Close-up of vesicles in the blue box in panel C. **C)** Full field of view of vesicles produced by gentle hydration. As expected, the sample predominantly contains multilamellar vesicles and nested vesicles. When contrast is optimized for the bright, multi-layered vesicles, unilamellar vesicles in the same field of view can be too dim to be imaged.

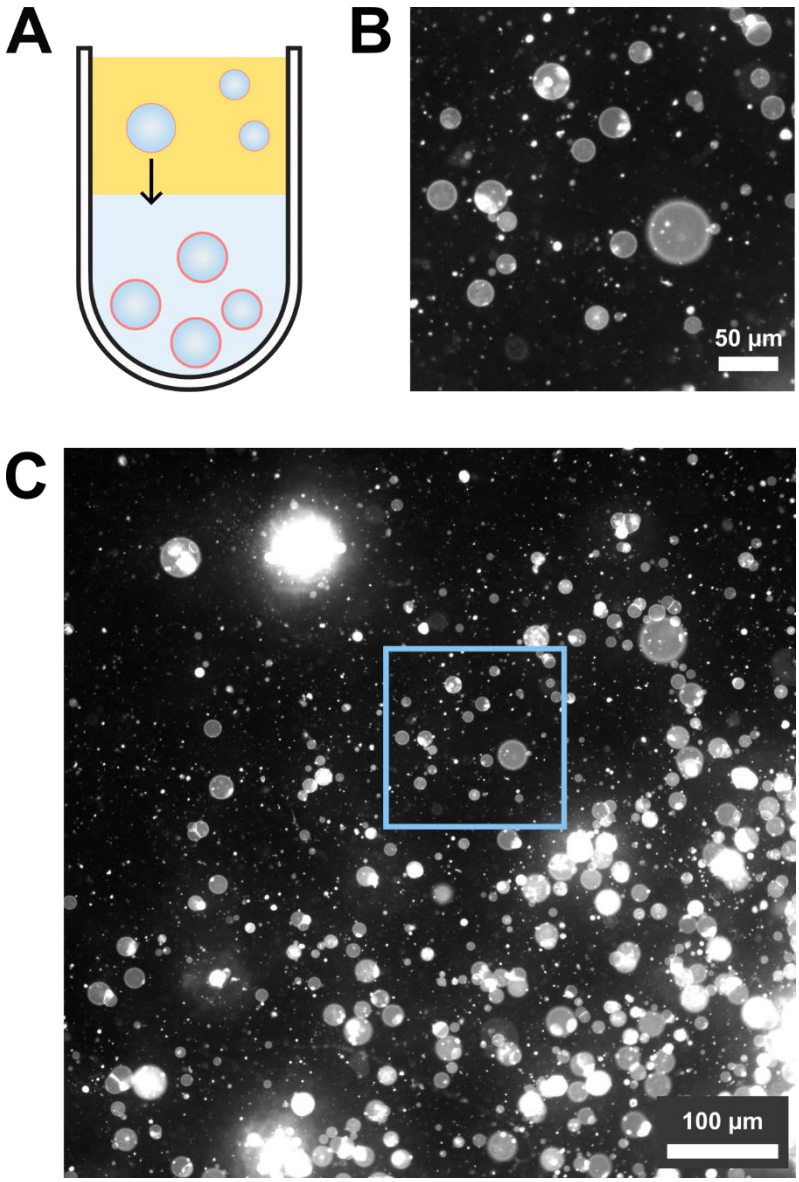

Figure S5. Representative fluorescence micrographs of vesicles made by emulsion phase transfer. A) Schematic of emulsion phase transfer. **B)** Close-up of vesicles in the blue box in panel C. **C)** Full field of view of vesicles produced by emulsion phase transfer. The emulsion transfer method produces a high yield of giant unilamellar vesicles as well as defects including nested vesicles and lipid aggregates.

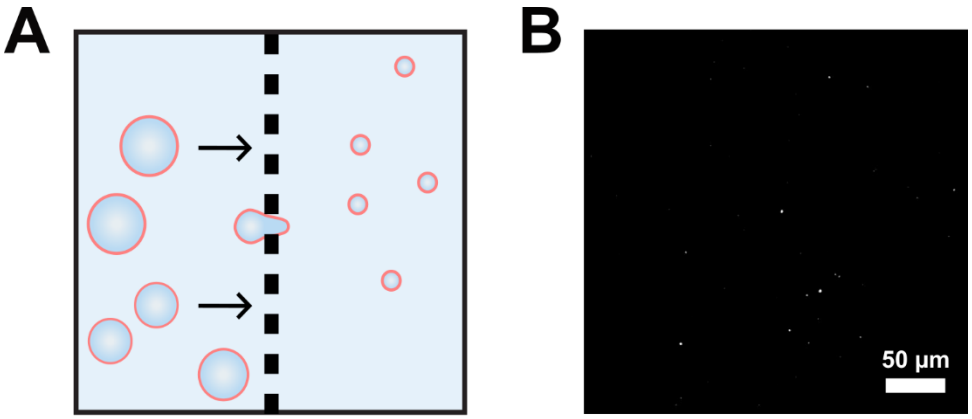

Figure S6. Vesicles after extrusion. A) Schematic of extrusion. **B)** Representative fluorescence micrograph of vesicles after extrusion through a 100 nm diameter membrane filter. As expected, most vesicles are too small to be resolved with standard microscopy.

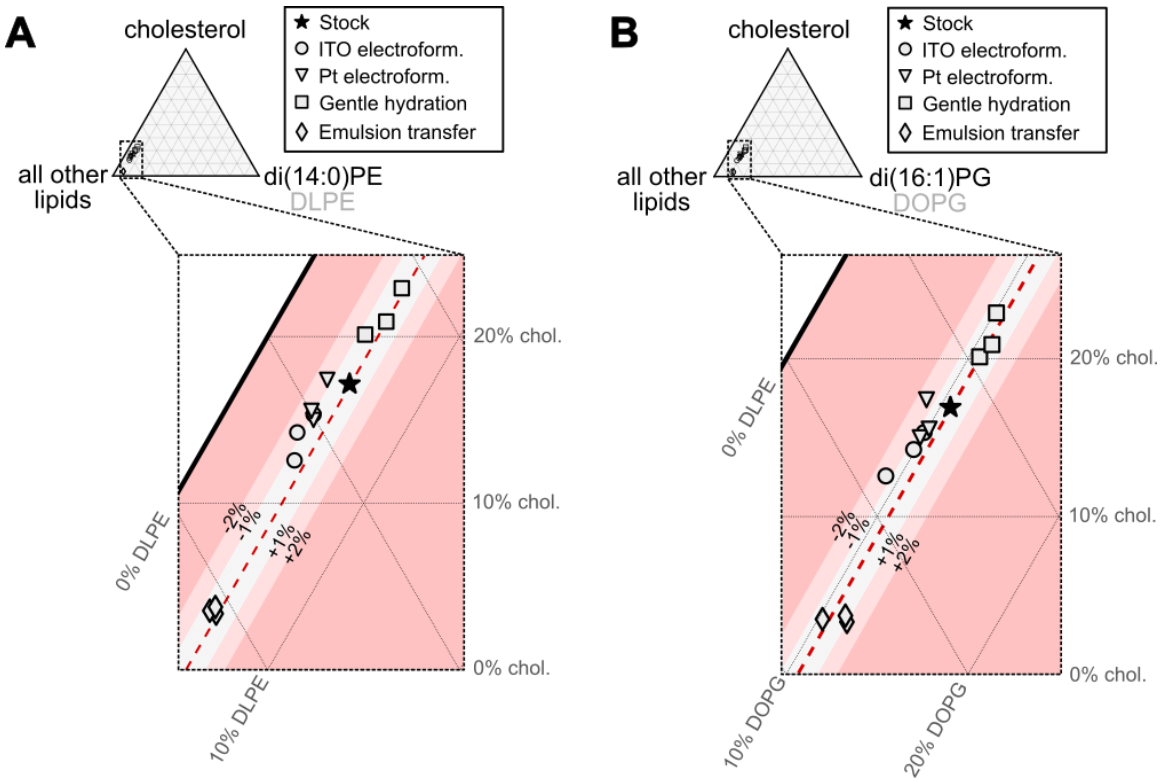

Figure S7. Lipid percentages in 5-component vesicles produced by different methods, plotted as pseudo-ternary diagrams in which one vertex is di(12:0)PE or di(18:1)PG. Vesicles were prepared by four methods: electroformation on ITO slides, electroformation on platinum wires, gentle hydration, and emulsion phase transfer. Three independent preparations and experiments were run for each method. **(A)** Lipid percentages of all solutions plotted on a pseudo-ternary diagram, where the three vertices represent di(12:0)PE, cholesterol, and the sum of all other lipids. **(B)** Lipid percentages of all solutions plotted on a pseudo-ternary diagram, where the three vertices represent di(18:1)PE, cholesterol, and the sum of all other lipids. In both panels, the lipid percentages for the master stock solution are shown as a star. Deviations from the master stock solution in increments of 1% and 2% of DLPE or DOPG are shown as shaded regions.

		Percentage of total lipid				
Method	Sample	Cholesterol	di(16:0)PC (DPPC)	di(18:1)PC (DOPC)	di(12:0)PE (DLPE)	di(18:1)PG(DOPG)
Stock solution	Master stock	17.0%	28.4%	38.3%	5.8%	10.4%
ITO electroform.	ITO 1	14.2%	28.0%	43.4%	4.4%	9.9%
	ITO 2	15.3%	28.1%	41.9%	4.7%	9.9%
	ITO 3	12.6%	29.5%	43.6%	5.1%	9.2%
Pt electroform.	Pt 1	17.4%	28.5%	40.7%	4.4%	9.0%
	Pt 2	15.0%	29.2%	41.1%	4.9%	9.9%
	Pt 3	15.5%	30.1%	39.7%	4.5%	10.1%
Gentle hydration	GH 1	22.9%	26.1%	35.3%	5.5%	10.1%
	GH 2	20.1%	27.1%	37.1%	5.0%	10.6%
	GH 3	20.9%	26.3%	36.2%	5.7%	10.9%
Emulsion transfer	Emulsion 1	3.4%	44.0%	35.4%	5.7%	11.6%
	Emulsion 2	3.5%	45.9%	35.1%	5.2%	10.2%
	Emulsion 3	3.8%	42.1%	37.3%	5.4%	11.3%

Table S1. Lipid compositions of five-component vesicles analyzed by mass spectrometry, expressed as percentages of total lipid.

		Percentage of total lipid	
Method	Sample	di(16:0)PC	di(16:1)PC
Stock solution for lipid saturation experiments	Saturation stock	49.1%	50.9%
Emulsion transfer (ET)	ET saturation 1	58.2%	41.8%
	ET saturation 2	58.0%	42.0%
	ET saturation 3	57.3%	42.7%

Table S2. Percentages of lipids in GUVs made by emulsion transfer from a binary mixture of an unsaturated lipid and a saturated lipid.

		Percentage of total lipid	
Method	Sample	di(18:1)PC	di(16:1)PC
Stock solution for lipid length experiments	Length stock	49.1%	50.9%
Emulsion phase transfer (ET)	ET length 1	58.8%	41.2%
	ET length 2	58.7%	41.3%
	ET length 3	53.1%	46.9%

Table S3. Percentages of lipids in GUVs made by emulsion transfer from a binary mixture of lipids with different chain lengths.

		Percentage of total lipid				
Method	Sample	Cholesterol	di(16:0)PC (DPPC)	di(18:1)PC (DOPC)	di(12:0)PE (DLPE)	di(18:1)PG (DOPG)
Before extrusion	Experiment 1 - Before	23.6%	25.2%	29.2%	6.9%	15.0%
	Experiment 2 - Before	26.3%	26.5%	25.6%	6.5%	15.1%
	Experiment 3 - Before	27.7%	25.8%	25.2%	6.3%	14.9%
After extrusion	Experiment 1 - After	18.0%	27.9%	32.1%	5.2%	16.9%
	Experiment 2 - After	22.4%	27.3%	27.1%	6.7%	16.6%
	Experiment 3 - After	22.3%	27.0%	28.4%	6.7%	15.6%

Table S4. Lipid compositions analyzed by mass spectrometry and expressed as percentages of total lipid for vesicles produced by gentle hydration ("before extrusion") and then extruded ("after extrusion"). For example, "Experiment 1 – After" was made from an aliquot of the solution from "Experiment 1 – Before".

Lipid	di(15:0)PC (internal standard)	di(16:0)PC	di(18:1)PC	di(15:0)PE (internal standard)	di(12:0)PE	di(15:0)PG (internal standard)	di(18:1)PG
m/z	706.5	734.6	786.6	686.5	602.4	717.5	797.5
Retention time (minutes)	3.467	3.467	3.414	2.725	2.847	0.708	0.621
Calibrated retention time (minutes)	6.760	6.760	6.672	5.542	5.742	2.233	2.038
Collisional cross section ($Å^2$)	274.4	279.8	285.1	268.9	252.5	268.6	279.4
Master stock abundance	5617.5	17245.3	23270.3	4528.2	2853.3	4441.4	5016.5
ITO electroform. 1 abundance	6741.8	17442.6	27025.4	4434.9	1810.2	5385.0	4914.3
ITO electroform. 2 abundance	6857.4	24043.3	35779.5	4280.0	2523.2	5170.9	6393.5
ITO electroform. 3 abundance	7240.7	15652.1	23118.4	4920.6	1843.7	6871.4	4625.1
Pt. electroform. 1 abundance	6881.0	22694.3	32436.7	4665.2	2379.2	5772.2	6026.1
Pt. electroform. 2 abundance	6679.0	16801.5	23631.0	5039.4	2124.3	6748.9	5740.9
Pt. electroform. 3 abundance	5342.4	14477.7	19085.5	4548.3	1847.1	5020.5	4557.4
Gentle hydration 1 abundance	7353.0	30264.4	40917.1	5487.3	4792.2	5907.4	9413.3
Gentle hydration 2 abundance	7682.1	23456.5	32112.9	6630.8	3748.8	5247.5	6246.9
Gentle hydration 3 abundance	7625.5	22749.8	31393.1	5379.8	3504.5	5017.3	6195.7
Emulsion transfer 1 abundance	8370.8	9579.3	7712.5	5534.3	816.3	6091.2	1843.4
Emulsion transfer 2 abundance	8068.4	11843.5	9051.1	5553.9	931.3	5927.0	1931.0
Emulsion transfer 3 abundance	7626.0	9787.1	8667.5	5246.7	867.2	5531.6	1910.8

Table S5. Phospholipid abundances of five-component vesicles analyzed by mass spectrometry.

	d7-cholesterol area (internal standard)	Cholesterol area
Master stock	3.21E+07	8.59E+06
ITO electroform. 1	2.68E+07	5.13E+06
ITO electroform. 2	2.76E+07	7.67E+06
ITO electroform. 3	2.53E+07	3.39E+06
Pt electroform 1	2.84E+07	8.33E+06
Pt electroform 2	2.61E+07	4.91E+06
Pt electroform 3	2.62E+07	5.33E+06
Gentle hydration 1	2.99E+07	1.57E+07
Gentle hydration 2	2.71E+07	8.93E+06
Gentle hydration 3	2.33E+07	8.05E+06
Emulsion transfer 1	2.23E+07	2.85E+05
Emulsion transfer 2	2.35E+07	3.88E+05
Emulsion transfer 3	3.67E+07	6.13E+05

Table S6. Cholesterol abundances of five-component vesicles analyzed by mass spectrometry.

Lipid	di(15:0)PC (internal standard)	di(16:0)PC	(16:0/18:1)PC (internal standard)	di(16:1)PC
m/z	706.5	734.6	760.6	730.5
Retention time (minutes)	3.312	3.312	3.259	3.414
Calibrated retention time (minutes)	5.445	5.445	5.453	5.429
Collisional cross section (Å2)	239.9	249.9	248.7	240.9
Saturation stock abundance	14259.5	490722.3	12208.1	434934.4
ET saturation 1 abundance	54941.2	45862.2	52621.1	31490.8
ET saturation 2 abundance	58862.0	21123.8	55943.2	14554.5
ET saturation 3 abundance	57614.3	39973.9	54335.7	28099.2

Table S7. Phospholipid abundances in GUVs made by emulsion transfer from a binary mixture of an unsaturated lipid and a saturated lipid.

Lipid	(16:0/18:1)PC (internal standard)	di(16:1)PC	di(18:1)PC
m/z	760.6	730.5	786.6
Retention time (minutes)	3.259	3.414	3.225
Calibrated retention time (minutes)	5.453	5.429	5.459
Collisional cross section (Å^2)	248.7	240.9	254.0
Length stock abundance	8362.4	428416.6	412967.2
ET length 1 abundance	51197.1	13380.6	19090.4
ET length 2 abundance	53042.6	5718.8	8128.1
ET length 3 abundance	54721.9	10486.8	11892.0

Table S8. Phospholipid abundances in GUVs made by emulsion transfer from a binary mixture of lipids with different chain lengths.

Lipid	di(15:0)PC (internal standard)	di(16:0)PC	di(18:1)PC	di(15:0)PE (internal standard)	di(12:0)PE	di(15:0)PG (internal standard)	di(18:1)PG
m/z	706.5	734.6	786.6	664.5	580.4	717.5	797.5
Retention time (minutes)	3.312	3.312	3.225	2.570	2.692	0.674	0.553
Calibrated retention time (minutes)	5.445	5.445	5.459	5.560	5.541	2.233	2.020
Collisional cross section (Å^2)	239.9	249.9	254.0	232.0	216.8	239.8	248.4
Before extrusion 1 abundance	56822.3	84583.4	97994.1	85471.0	34719.6	36543.5	32416.2
Before extrusion 2 abundance	63191.0	113815.1	109639.1	101636.3	44984.7	39897.5	40816.1
Before extrusion 3 abundance	63430.2	159911.8	156115.9	95764.3	59014.5	30611.1	44526.0
After extrusion 1 abundance	54683.8	32544.4	37473.0	89296.3	9911.4	43706.7	15788.9
After extrusion 2 abundance	65041.1	65510.5	65082.1	96925.9	23877.9	37763.1	23185.0
After extrusion 3 abundance	50216.3	63415.0	66752.6	85189.5	26663.7	36801.5	26753.6

Table S9. Phospholipid abundances in GUVs produced by gentle hydration ("before extrusion") and then extruded ("after extrusion"). For example, "After extrusion 1" was made from an aliquot of the solution from "Before extrusion 1".

Sample	Cholesterol area	d7-cholesterol area (internal standard)
Master stock	3.88E+08	1.61E+07
Before extrusion 1	4.26E+06	1.70E+07
Before extrusion 2	5.44E+06	1.69E+07
Before extrusion 3	8.02E+06	1.65E+07
After extrusion 1	1.09E+06	1.58E+07
After extrusion 2	2.47E+06	1.66E+07
After extrusion 3	2.89E+06	1.54E+07

Table S10. Cholesterol abundances in GUVs produced by gentle hydration ("before extrusion") and then extruded ("after extrusion"). For example, "After extrusion 1" was made from an aliquot of the solution from "Before extrusion 1".